Int. J. Heat Mass Transfer. Vol. 27, No. 2, pp. 291–300, 1984
Printed in Great Britain

0017 9310/84 $3.00 + 0.00

EXTINCTION OF PREMIXED FLAMES BY STRETCH AND RADIATIVE LOSS

S. H. SOHRAB and C. K. LAW
Department of Mechanical and Nuclear Engineering, Northwestern University, Evanston, IL 60201, U.S.A.

(*Received* 22 *March* 1983 *and in revised form* 1 *June* 1983)

Abstract—The extinction of laminar premixed flames by stretch and radiative loss is studied for the model problem of counterflow opposed-jet combustion by using the matched asymptotic expansion technique for the highly temperature sensitive processes of radiative heat loss and large-activation-energy reaction kinetics. Explicit expressions for the critical Damköhler number at extinction are derived and the influence of upstream vs downstream heat losses assessed. Results show that stretch exerts a much stronger influence than radiative loss on flame extinction.

NOMENCLATURE

- a — $\gamma_{jf}T_f/T_a$
- B — frequency factor
- C_p — specific heat at constant pressure
- D — mass diffusion coefficient
- Da — Damköhler number, equation (3)
- E — activation energy
- F — radiative heat loss per unit volume per unit time divided by $\rho\Gamma Q$
- $G^{\pm}$ — temperature gradients, equations (26) and (27)
- g — coefficient defining temperature sensitivity of γ, d(ln γ)/(ln T)
- H — strength of chemical heat source, equation (15)
- k — flow factor (1, two-dimensional; 2, axisymmetric)
- Le — Lewis number, $\lambda/(C_p\rho D)$
- l_p — Planck-mean absorption length
- M — molecular weight
- m — temperature gradient parameter, equation (36)
- n — parameter defined in equation (50)
- P — parameter defined in equation (44)
- p — parameter defined in equation (39)
- Q — heat of combustion (fuel-mass based)
- q — total nondimensional radiative heat loss, equation (18)
- R — gas constant
- r — traverse coordinate
- T — nondimensional temperature
- T_a — nondimensional activation temperature, $EC_p/(RQ)$
- T_{fa} — adiabatic flame temperature
- u — tangential velocity
- u_e — freestream velocity
- W — reaction rate, equation (4)
- x — canonical coordinate, equation (7)
- Y — stoichiometrically adjusted mass fraction
- Y_{Ou} — freestream oxygen mass fraction
- y — stretched coordinate, $(x-x_f)(\alpha/x_f)(T_a/T_f^2)$
- z — nondimensional axial coordinate.

Greek symbols

- α — $Y_{Ou}/\nu Y_{Fu}$
- β — effective difference between downstream and upstream nondimensional temperatures
- Γ — rate of strain, $k(du_e/dr)$
- γ — coefficient defining temperature sensitivity of $F(T)$, d(ln F)/d(ln T)
- Δ — radiative loss parameter, equation (24)
- δ — Dimrac's delta function
- ε — small parameter, T_f^2/T_a
- η — stretched coordinate, $y-p_0/m$
- θ — stretched temperature, $(T_f-T)T_a/T_f^2$
- Λ — radiative loss parameter, equation (32)
- λ — gas thermal conductivity
- ν — stoichiometric mass ratio of oxidizer to fuel
- ξ — stretched coordinate, equation (22)
- ρ — density
- σ — Stefan–Boltzmann constant
- τ — stretched temperature, $\theta-(m\eta+p_0)$
- ϕ — stretched temperature, equation (20)
- ψ — coupling function, $(Y_O+T-T_f)T_a/T_f^2$
- Ω — reduced Damköhler number, equation (33).

Subscripts

- a — activation
- b — burnt mixture
- c — critical
- F — fuel
- f — flame
- i — F or O
- j — u or b
- u — unburnt mixture.

1. INTRODUCTION

ANALYTICAL studies on radiative transfer in combustion processes are relatively few compared with those for convective and diffusive transfer. This apparent imbalance in emphases is partly due to the analytical difficulty caused by the strong non-linearity associated with the physical laws governing radiative transfer. Furthermore, either by nature or design, laboratory flames are usually relatively small such that the long-range radiative effects tend to have secondary importance compared with those due to convective and diffusive transport. Thus analytical modeling of these laboratory flames frequently neglect radiation.

However, there exist strong incentives, from both the practical and fundamental viewpoint, to gain an improved understanding of radiative effects in combustion processes. For example, since the optical thickness representing the length scale associated with radiative transport is often much larger than the flame thickness relevant to conductive–convective transports, radiation could be the dominant heat transfer mechanism in large-scale real situation fires [1] such as the flame spreading and flashover phenomena in fire research, and heat transfer in furnaces and boilers. Furthermore, with the anticipated emphasis on the utilization of the aromatics-rich synthetic fuels which have strong propensity to produce soot upon combustion, the increased radiative transfer will aggravate the extent of thermal stress experienced by the combustion chamber.

From the fundamental viewpoint, the presence of radiation can greatly enrich the physical phenomena of certain combustion systems. For example, radiative transfer in flames primarily depends on the absolute values of the temperature rather than the temperature gradients associated with the convective and diffusive transport. The spectral emission/absorption of radiation in gases can also result in selective heat loss/gain, a phenomenon which is totally absent in other modes of energy transport.

Quantitatively, as a result of the high temperature sensitivity of the reaction rate, it may also be expected that there exist situations under which the influences of radiative heat loss can become comparable with the convective–diffusive losses and thereby change the extinction behavior of even small-scale flames. An interesting example is the recent experimental result of Ishizuka and Law [2] which seems to indicate that downstream radiative loss promotes the extinction of a rich propane/air premixed flame.

The radiative extinction of diffusion flames has been previously studied using matched asymptotic analysis for large reduced activation energy and the temperature coefficient of the radiant loss [3]. In the present paper this study is extended to the system of premixed flames. It is reasonable to expect that radiative loss may exert different influences on these two flames in that while the nature of chemical reactivity and radiative loss are somewhat symmetrical in the fuel and oxidizer sides of a diffusion flame, in a premixed flame the upstream is reactive but mostly cold and hence less radiative, while the downstream is non-reactive but mostly hot and hence more radiative. Thus the influence of upstream vs downstream radiative losses on chemical reactivity is unclear.

The premixed flame system adopted for study is that of the axisymmetric counterflow, which exerts a well-defined stretch rate on the flame. The interest in studying the behavior of a stretched flame is that stretch is recognized as an important mechanism in causing extinction [4]. Since radiative heat loss is always present, and is especially significant at the rich extinction limit, it is necessary to examine the extent by which the critical extinction conditions may be modified by allowing for radiative loss.

The problem is formulated in the next section, which is followed by analysis of the thin radiative loss zone and then the much thinner reaction zone. An explicit extinction criterion is derived and influences due to upstream vs downstream losses are identified. The reader is also referred to ref. [1] for a recent review of the various aspects of radiative heat transfer in combustion systems.

2. FORMULATION

The conservation equations for energy and the reactant concentrations for the axisymmetric counterflow considered here are [3]

$$z\frac{dT}{dz}+\frac{d^2T}{dz^2}=-W(Y_O,Y_F,T)+F(T), \tag{1}$$

$$z\frac{dY_i}{dz}+\frac{d^2Y_i}{dz^2}=W(Y_O,Y_F,T),\quad i=O,F. \tag{2}$$

Here z is the axial coordinate nondimensionalized with the characteristic length for the mixing layer $\sqrt{(\Gamma/D)}$, $\Gamma=k(du_e/dr)$ is the rate of strain, and $D=D_O=D_F$ is the diffusion coefficient which is assumed constant. The Lewis number, $Le=\lambda/(C_p\rho D)$, is taken to be unity; where λ, ρ and C_p denote the gas thermal conductivity, density and specific heat at constant pressure, respectively. The flame is established in a viscous layer produced between the opposing streams of fuel/oxidizer mixture approaching from $z=+\infty$ and an inert gas from $z=-\infty$. Temperature T is made nondimensional by $C_p/(QY_{Fu})$, where Y_{Fu} and Q denote the fuel mass fraction in the unburnt stream and the heat of combustion per unit mass of fuel, respectively. The concentrations Y_O and Y_F are the oxidizer and fuel mass fractions divided by νY_{Fu} and Y_{Fu}, respectively, with ν denoting the stoichiometric mass ratio of oxidizer to fuel. $W(Y_O,Y_F,T)$ is a nondimensional chemical reaction rate and $F(T)$ the radiative heat loss per unit volume per unit time divided by $\rho Q\Gamma$.

A one-step irreversible reaction which is of order unity with respect to both fuel and oxidizer is considered. In terms of an appropriate Damköhler number Da, which represents the ratio of characteristic flow to chemical reaction times

$$Da=\frac{B\rho Y_{Fu}}{M_F\Gamma}, \tag{3}$$

the reaction rate following Arrhenius kinetics is expressed by

$$W=(Da)Y_OY_F\exp(-T_a/T), \tag{4}$$

where T_a is the nondimensional activation energy, B is the frequency factor, and M_F is the fuel molecular weight.

Equations (1) and (2) are subject to the following boundary conditions:

$$\begin{aligned} z &= +\infty, \quad T-T_\infty = Y_F-1 = Y_O-\alpha = 0, \\ z &= -\infty, \quad T-T_{-\infty} = Y_O = Y_F = 0, \end{aligned} \tag{5}$$

where $\alpha = Y_{Ou}/(\nu Y_{Fu})$ and Y_{Ou} is the oxidizer mass fraction in the unburnt mixture.

Treatment of radiative losses assumes an optically thin gas, hence reabsorption of radiation by the emitting gas is neglected. Such an assumption is reasonable for the small-scale flames being considered [5, 6]. Since the penetration depth of an optical beam is much larger than the characteristic flame lengths, the hot gas consequently loses heat by thermal radiation to an infinite surrounding sink. In this optically thin limit, the rate of radiative energy loss per unit volume is $4\sigma(TQY_{Fu}/C_p)^4/l_p$, where σ and l_p denote the Stefan–Boltzmann constant and the Planck mean absorption length, respectively [7]. The radiative loss term, $F(T)$, is then expressed as

$$F(T) = \frac{4\sigma(TQY_{Fu}/C_p)^4}{l_p \rho Q \Gamma}. \tag{6}$$

Noting that $\rho \sim T^{-1}$, the above expression shows that in the absence of any temperature dependence of l_p, $F(T)$ is proportional to T^5. As discussed previously by Sohrab *et al.* [3], l_p typically decreases with increasing temperature. This then results in temperature exponents even larger than five for $F(T)$. We also note that with the realistic assumption of an optically thin gas, the total radiative loss is proportional to the volume of the hot emitting gases. Therefore, in premixed systems where the entire downstream region is mostly, if not entirely, composed of hot combustion products, the total radiative loss could be more significant compared with the diffusion flames.

Convection-free forms of equations (1) and (2) can be obtained by the introduction of a new independent variable [8]

$$x = 1/2\,\mathrm{erfc}(z/\sqrt{2}). \tag{7}$$

In terms of x, equations (1) and (2) become

$$\frac{d^2T}{dx^2} = -2\pi\{\exp(z^2)\}W + 2\pi\{\exp(z^2)\}F(T), \tag{8}$$

$$\frac{d^2Y_i}{dx^2} = 2\pi\{\exp(z^2)\}W, \quad i = \mathrm{O}, \mathrm{F}, \tag{9}$$

which are bounded in the range $0 \leqslant x \leqslant 1$. The boundary conditions are

$$\begin{aligned} x &= 0: \quad T-T_\infty = Y_F-1 = Y_O-\alpha = 0, \\ x &= 1: \quad T+\beta-T_\infty = Y_F = Y_O = 0, \end{aligned} \tag{10}$$

where $\beta = T_\infty - T_{-\infty}$. The two streams are assumed to have equal velocities such that the stagnation plane occurs at $x = 1/2$ when $\beta = 0$ and $\rho_\infty = \rho_{-\infty}$. Extension of the solution to the adiabatic (downstream) boundary condition at $x = 1/2$ is presented in the Appendix.

In the limit $T_a \to \infty$, chemical reaction will be confined to an infinitesimally-thin reaction zone located at the maximum temperature. The solution for the concentration of the oxidizer, which is assumed to be the deficient, and thereby controlling, specie is readily obtained from equation (9) as

$$Y_O = \alpha - \alpha(x/x_f), \quad x \leqslant x_f, \tag{11}$$

and

$$Y_O = 0, \quad x \geqslant x_f. \tag{12}$$

Furthermore, since radiation loss is negligible within this reaction zone, the first integral of equations (8) and (9) shows that the jump conditions for the temperature and species gradients across the reaction zone are related by

$$\left[\frac{dT}{dx}\right]_-^+ + \left[\frac{dY_O}{dx}\right]_-^+ = 0, \tag{13}$$

where $[f]_-^+ = f(\mathrm{O}^+) - f(\mathrm{O}^-)$, and the + and − signs refer to the burnt and unburnt sides of the reaction zone, respectively.

In equation (9), the reaction term can be expressed as a delta function, $\delta(x)$, in the present limit, the strength of which is obtained by evaluating the first integral of

$$\frac{d^2Y_O}{dx^2} = H\delta(x-x_f), \tag{14}$$

across the reaction zone with the use of the solution (11) and (12). Thus

$$H = \left[\frac{dY_O}{dx}\right]_-^+ = -\left[\frac{dT}{dx}\right]_-^+ = \frac{\alpha}{x_f}, \tag{15}$$

where equation (13) has been applied to show the relations between H and the jump in the gradients of Y_O and T.

Furthermore, since $F(T)$ is also a sensitive function of temperature as just discussed, the radiative loss zone will be confined to a thin region embedding the much thinner reaction zone; its characteristics will be quantified in Section 3. Therefore away from these regions of the highest temperature, both chemical reaction and radiative loss can be neglected. Then equation (8) has the solution

$$T = T_\infty + (T_f - T_\infty)\frac{x}{x_f}, \quad x \leqslant x_f, \tag{16}$$

$$T = T_\infty - \beta + (T_f + \beta - T_\infty)\left(\frac{1-x}{1-x_f}\right), \quad x \geqslant x_f. \tag{17}$$

The flame temperature, T_f, which is smaller than the adiabatic flame temperature, can be determined by relating it to the strengths of the chemical heat source and the radiative heat sink. Thus with the radiative loss term in equation (8) represented by a delta function of strength q, the first integral of equation (8) and the results of equations (16) and (17) give the total energy loss by radiation as

$$q = \frac{\alpha}{x_f} - \left\{\left(\frac{T_f+\beta-T_\infty}{1-x_f}\right) + \left(\frac{T_f-T_\infty}{x_f}\right)\right\}. \quad (18)$$

Equation (18) relates the total radiative loss to the total chemical heat release and the slopes of the temperature distributions on both sides of the radiative zone. However, equation (18) does not relate T_f and x_f to the heat loss function $F(T)$; to obtain such a relation requires analysis of the radiation zone which follows.

3. RADIATION ZONE ANALYSIS

The strong temperature dependence of $F(T)$ can be represented in terms of a large parameter γ defined as

$$\gamma = \frac{\mathrm{d}(\ln F)}{\mathrm{d}(\ln T)} \gg 1, \quad (19)$$

such that $F \sim T^\gamma$ when γ is assumed to be constant. Since the radiation characteristics of the gas before and after combustion are different, γ_u and γ_b will be used to distinguish the unburnt and burnt sides of the reaction zone, respectively. The temperature dependence of γ_j, $j = \mathrm{u,b}$, is assumed to be weak such that $g_j = \mathrm{d}(\ln \gamma_j)/\mathrm{d}(\ln T)$ is an order one quantity. For large γ_j, the contributions to radiative losses come primarily from the high temperature regions in the vicinity of flame temperature T_f. Thus in terms of a new dependent variable defined as

$$\phi = \left(\frac{T-T_f}{T_f}\right)\gamma_{jf}, \quad (20)$$

an asymptotic expansion of $F(T)$ in powers of γ_{jf}^{-1} for ϕ of order unity can be shown to be [3]

$$F(T) = F_f \mathrm{e}^\phi\left[1+\frac{g_{jf}-1}{2\gamma_{jf}}\phi^2+,\ldots\right], \quad (21)$$

where the subscript f denotes quantities evaluated at the flame temperature T_f.

For analysis of the thin radiative zone the stretched coordinate ξ defined as

$$\xi = \frac{(x-x_f)}{T_f}\gamma_{jf}, \quad (22)$$

is introduced. Thus the structure of the radiative zone is given by the first-order approximation of equation (8) for large γ_{jf}

$$\frac{\mathrm{d}^2\phi}{\mathrm{d}\xi^2} = \Delta_j \mathrm{e}^\phi - \frac{\alpha}{x_f}\delta(\xi), \quad (23)$$

where $\delta(\xi)$ is the delta function. The radiative loss parameter, Δ_j, appearing in equation (23), is the ratio of a Bouguer number to a Boltzmann number [7] and depends on the flame temperature and position through

$$\Delta_j = 2\pi\frac{T_f}{\gamma_{jf}}F_f \exp(z_f^2), \quad j = \mathrm{b,u}. \quad (24)$$

In view of the definitions of F_f, Δ_j represents the ratio of the rate of radiative energy loss to that for the convection of enthalpy. This parameter may also be viewed as the ratio of the characteristic residence time to the characteristic radiative emission time.

The boundary conditions for equation (23) are obtained from matching with the outer, adiabatic and chemically frozen solutions given by equations (16) and (17)

$$\begin{aligned} \xi \to -\infty, \quad \frac{\mathrm{d}\phi}{\mathrm{d}\xi} &= \frac{T_f-T_\infty}{x_f}, \\ \xi \to +\infty, \quad \frac{\mathrm{d}\phi}{\mathrm{d}\xi} &= -\frac{T_f+\beta-T_\infty}{1-x_f}. \end{aligned} \quad (25)$$

The first integral of equation (23) on either side of the reaction zone, from $\xi \to \pm\infty$ to $\xi = 0^\pm$, result in

$$G^- \equiv \left.\frac{\mathrm{d}\phi}{\mathrm{d}\xi}\right|_{0^-} = \left[2\Delta_u + \left(\frac{T_f-T_\infty}{x_f}\right)^2\right]^{1/2}, \quad (26)$$

$$G^+ \equiv \left.\frac{\mathrm{d}\phi}{\mathrm{d}\xi}\right|_{0^+} = -\left[2\Delta_b + \left(\frac{T_f+\beta-T_\infty}{1-x_f}\right)^2\right]^{1/2}, \quad (27)$$

where + and − refer to $\xi \gtrless 0$. The quantities G^+ and G^- represent the slopes of the temperature distributions on the burnt and unburnt sides of the flame, respectively. Using the jump condition across the reaction zone from equation (15), with the results in equations (26) and (27), one obtains

$$\left[2\Delta_b + \left(\frac{T_f+\beta-T_\infty}{1-x_f}\right)^2\right]^{1/2} + \left[2\Delta_u + \left(\frac{T_f-T_\infty}{x_f}\right)^2\right]^{1/2} = \frac{\alpha}{x_f}, \quad (28)$$

which relates the heat loss parameters to the nonadiabatic flame temperature and location. In the absence of radiative heat loss, $\Delta_j = 0$, then T_{fa} and x_{fa} are related by equation (28) through

$$x_{fa} = \frac{\alpha+T_\infty-T_{fa}}{\alpha+\beta}, \quad (29)$$

which is the expected adiabatic result. Equations (26) and (27) indicate that radiative loss tends to steepen the temperature gradients on either side of the reaction zone. This in turn enhances the tendency towards extinction by promoting the conductive loss and shortening the residence time. A schematic of the temperature distribution is shown in Fig. 1(a).

The problem is as yet not closed in that equation (28) is insufficient to uniquely determine x_f and T_f. The additional information is to be provided by an analysis of the reaction zone structure, to be presented next.

4. REACTION ZONE ANALYSIS

In the realistic limit [3] of $T_f/\gamma_{jf} \gg T_f^2/T_a$, the thin reaction zone is embedded within the relatively broader radiation zone. The small parameter $\varepsilon = T_f^2/T_a$ is used

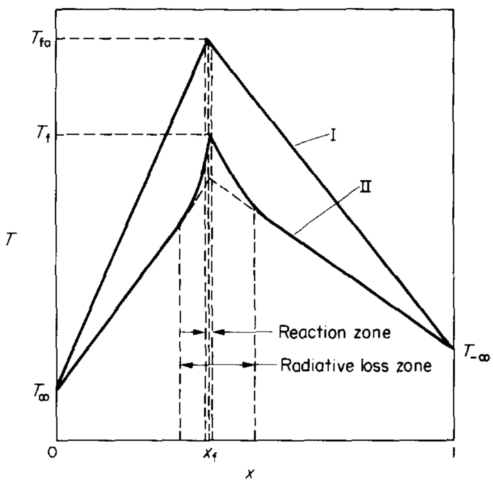

FIG. 1(a). Schematic diagram of the temperature distributions for: (I) adiabatic single flame; (II) nonadiabatic single flame.

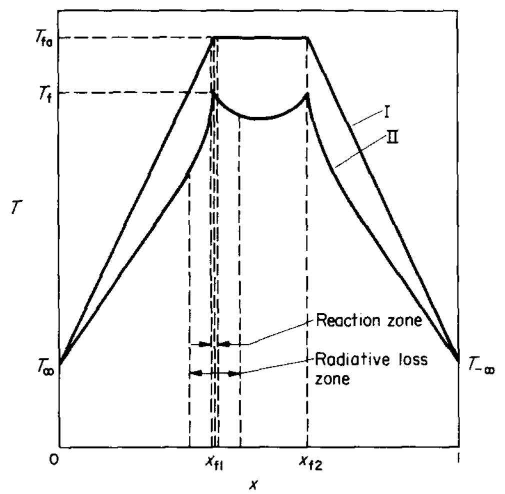

FIG. 1(b). Schematic diagram of the temperature distribution for: (I) adiabatic double flames; (II) nonadiabatic double flames.

to define the stretched coordinate and temperature as

$$y = (x - x_f)\left(\frac{\alpha}{x_f}\right)(T_a/T_f^2),$$

and

$$\theta = (T_f - T)(T_a/T_f^2).$$

In terms of the coupling function

$$\psi = (Y_O + T - T_f)T_a/T_f^2,$$

from equations (8) and (9) we obtain

$$\frac{d^2\psi}{dy^2} = \Lambda\, e^{-a\theta}, \tag{30}$$

$$\frac{d^2\theta}{dy^2} = \Omega(\psi + \theta)e^{-\theta} - \Lambda\, e^{-a\theta}, \tag{31}$$

where $a = \gamma_{jf} T_f/T_a$ signifies the relative value of the temperature sensitivity for the radiation and chemical reaction processes.

The factors Λ and Ω, which denote a radiative loss parameter and a reduced Damköhler number, respectively, are given by

$$\Lambda = 2\pi(x_f/\alpha)^2(T_f^2/T_a)F_f\{\exp(z_f^2)\}, \tag{32}$$

$$\Omega = 2\pi(x_f/\alpha)^2\, Da\, Y_{Ff}(T_f^2/T_a)^2\{\exp(z_f^2 - T_a/T_f)\}, \tag{33}$$

where Y_{Ff} is the fuel mass fraction within the reaction zone. The boundary conditions for equations (30) and (31) are obtained from matching as

$$\frac{d\theta}{dy} = -\frac{d\psi}{dy} = \left(\frac{T_f + \beta - T_\infty}{1 - x_f}\right)\left(\frac{x_f}{\alpha}\right), \quad y \to \infty, \tag{34}$$

$$-\frac{d\theta}{dy} = 1 + \frac{d\psi}{dy} = \frac{T_f - T_\infty}{\alpha}, \quad y \to -\infty. \tag{35}$$

In general, solutions of equations (30) and (31) subject to the above boundary conditions will require numerical integration. In the present limit of the thin reaction zone compared with the radiative loss zone, the boundary conditions for equation (31) are given by equations (26) and (27). We introduce the parameter defined by

$$m = \frac{x_f}{\alpha}\left[2\Delta_b + \left(\frac{T_f + \beta - T_\infty}{1 - x_f}\right)^2\right]^{1/2}, \tag{36}$$

where in view of equation (28), the quantity $(m-1)/m$ is the ratio of the slope of the temperature profiles on the burnt and unburnt sides of the reaction zone. The boundary conditions (34) and (35) can be expressed as

$$\frac{d\theta}{dy} = m, \quad y \to +\infty, \tag{37}$$

$$\frac{d\theta}{dy} = m - 1, \quad y \to -\infty. \tag{38}$$

In the first approximation, setting $\Lambda = 0$, the equations for ψ and θ decouple and the solution of equation (30) is given by $\psi = \psi_f + by$, where ψ_f and b are constants of integration. Matching of the slopes with those from the outer solution

$$\frac{dY_O}{dx} = 0 \text{ as } y \to +\infty,$$

and

$$\frac{dY_O}{dx} = -\frac{\alpha}{x_f} \text{ as } y \to -\infty,$$

gives $d\psi/dy = -m$ as $y \to \pm\infty$ and thus $b = -m$. Since $O(1)$ changes in ψ correspond to $O(\varepsilon)$ changes in T_f, T_f is chosen such that $\psi_f = 0$ resulting in the solution $\psi = -my$.

By introducing the factor

$$p = \ln(2\Omega), \tag{39}$$

and the corresponding expansion

$$p = p_0 + \varepsilon p_1 +, \ldots, \tag{40}$$

the new translated coordinate $\eta = y - p_0/m$ and modified inner temperature $\tau = \theta - (m\eta + p_0)$ are defined. In terms of these new quantities, equation (31) and the boundary conditions (37) and (38) will assume the simple form

$$2\frac{d^2\tau}{d\eta^2} = \tau \exp(-m\eta + \tau), \tag{41}$$

$$\frac{d\tau}{d\eta} = 0, \qquad \eta \to +\infty, \tag{42}$$

$$\frac{d\tau}{d\eta} = -1, \quad \eta \to -\infty. \tag{43}$$

Equation (41) subject to the boundary conditions (42) and (43) was previously solved by Liñán [8]; it was found to possess no solution when $m \geq 0.5$.

The fuel rich mixture being considered results in $O(1)$ and $O(\varepsilon)$ leakages of fuel and oxidizer across the reaction zone, respectively. The appropriate expansions for oxidizer mass fraction on each side of the reaction zone which satisfy the boundary conditions are

$$Y_O = \varepsilon P_1(1-x) + \varepsilon^2 P_2(1-x) + ,\ldots, \quad x > x_f, \tag{44}$$

$$Y_O = \alpha - \frac{\alpha}{x_f}x + \varepsilon P_1\left(\frac{1-x_f}{x_f}\right)x + ,\ldots, \quad x < x_f, \tag{45}$$

where continuity of Y_O across $x = x_f$ has been used. The gradient

$$\left(\frac{dY_O}{dx}\right)_{x=1} = -\varepsilon P_1 - \varepsilon^2 P_2, \ldots, \tag{46}$$

reflects $O(\varepsilon)$ leakage of the oxidizer through the flame.

By matching of the values for ψ as $\eta \to \pm\infty$, using the definition of m and τ and the results in equations (28), (47) and (48), we obtain

$$P_1(1-x_f) = \tau_\infty, \tag{47}$$

$$p_0 = -mn, \tag{48}$$

where the limiting quantities n and τ_∞ are defined as

$$\tau_\infty = \lim \tau, \quad \eta \to +\infty, \tag{49}$$

$$n = \lim(\tau + \eta), \quad \eta \to -\infty. \tag{50}$$

Equation (47) thus provides the amount of oxidizer leakage through the reaction zone. The fuel concentration within the reaction zone is obtained from the solution of equation (8) for $i = $ O, F

$$Y_F - Y_O = (1-\alpha)(1-x), \tag{51}$$

evaluated at $x = x_f$, $Y_O = 0$. We obtain

$$Y_{Ff} = (1-\alpha)(1-x_f), \tag{52}$$

which is to be used in equation (33).

Equation (48) after substitution from equations (33), (39) and (40) results in

$$Da = \frac{1}{4\pi}\{\exp(-z_f^2)\}(\alpha/x_f)^2(T_a/T_f^2)^2 Y_{Ff}^{-1} \times \exp(T_a/T_f - mn), \tag{53}$$

which is the desired expression relating the Damköhler number to the flame temperature, location and the heat loss parameters. Further substitution from equations (52) and (36) shows the explicit relationship between Da, T_f, x_f and Δ_j

$$Da = \frac{1}{4\pi}\{\exp(z_f^2)\}(\alpha T_a/x_f T_f^2)^2\left(\frac{1}{(1-\alpha)(1-x_f)}\right) \times \exp(T_a/T_f)\exp\left\{-\frac{nx_f}{\alpha}\left[2\Delta_b + \left(\frac{T_f+\beta-T_\infty}{1-x_f}\right)^2\right]^{1/2}\right\}. \tag{54}$$

More details on the structure of the reaction zone including plots of τ as a function of η for various values of the parameter m can be found in Liñán [8]. Moreover, appropriate expressions for the quantity (nm) in equation (53) have also been obtained [8], indicating that for $0.2 < m < 0.5$

$$nm = 1.344m - 4m^2(1-m)/(1-2m) + 3m^3 - \ln(1-4m^2), \tag{55}$$

and for small positive and all negative values of m

$$nm = -\ln(0.6307m^2 - 1.344m + 1). \tag{56}$$

For small m, the quantity n can be accurately approximated by 1.344 according to Liñán [8].

5. RESULTS AND DISCUSSION

For any specified flow field and overall reaction rate constant which describes Da, equations (24), (28) and (53) provide three relations to solve for Δ_j, x_f and T_f. An iterative procedure may be used where a flame temperature is assumed and the corresponding x_f and Δ_j are determined from equations (24) and (28). The results are then used in equation (53) to evaluate a new value for T_f. This process is repeated until the three equations are simultaneously satisfied. Numerical analysis of equation (53) yields the upper half of an S-shaped curve in the $(T_f - Da)$ plane, for a given value of Δ_j. A critical minimum value of Da, Da_E, is thus determined below which flames will extinguish as a result of reduced flame temperature and insufficient residence time for completion of reaction.

The critical value of $m = 0.5$, above which equations (41)–(43) have no solution, corresponds to equal slopes of the flame temperature profile on either side of the flame sheet. A critical heat loss parameter Δ_{bc} is defined to correspond to $m = 0.5$ and is determined from equations (36) and (28)

$$\Delta_{bc} = \frac{\alpha^2}{8(x_f^2)} - \frac{1}{2}\left(\frac{T_f+\beta-T_\infty}{1-x_f}\right)^2. \tag{57}$$

The following range for the downstream radiative loss parameter is thus identified

$$0 < \Delta_b < \Delta_{bc}. \tag{58}$$

Therefore, for any given flame location and temperature, a critical maximum radiative loss parameter, Δ_{bc}, exists above which flame propagation is no longer possible.

Equation (28) will result in an eighth-degree polynomial in terms of x_f for general values of Δ_j. For given Δ_j and varying T_f, the unique root of such a polynomial which is in the range

$$0 < x_f < 1/2, \tag{59}$$

and satisfies the condition of equation (58), has been numerically determined using the Newton–Raphson technique, with Δ_j being the appropriate heat loss parameter. It may also be noted that in the numerical evaluations the quantity $\exp(-z_f^2)$ can be approximated by an expression in terms of x_f as suggested by Liñán [8]

$$\exp(-z_f^2) = 2\pi x_f^2 \ln\left[\frac{(1+3.938x_f)}{2\pi x_f^2}\right], \tag{60}$$

where x_f is in the range $0 \leqslant x_f \leqslant 1/2$.

Plots of the flame temperature as a function of the Damköhler number for various fixed values of the heat loss parameter $\Delta = \Delta_j$ are shown in Fig. 2. To obtain such plots, values of $\Delta = 0.0, 0.1$, and 1.0 are substituted in equation (28) to obtain x_f for various T_f. The calculated x_f and the corresponding Δ and T_f are then used in equation (54) to determine Da. The remaining parameters of the problem α, β, T_a and T_u are also specified. As shown in Fig. 2, larger Δ corresponds to larger Da_E, indicating that the flames with larger heat loss will extinguish at larger residence times, as is to be expected.

The critical values of the flame temperature at extinction show a weak dependence on the parameter Δ (Fig. 2) which emphasizes the previous findings [8] that only $O(T_f^2/T_a)$ reduction in flame temperature is needed to achieve extinction. Consequently, larger radiative loss parameters mainly shift the extinction curves toward larger Damköhler numbers.

As seen in equations (26) and (27), the influence of radiative loss on the flame structure is through the appearance of Δ_j in the slopes of the temperature distribution on either side of the reaction zone. Clearly, neglect of either downstream or upstream heat loss will result in the vanishing of Δ_b or Δ_u in G^+ or G^-, respectively. Therefore, to evaluate the influences of the downstream vs upstream radiative loss, extinction curves corresponding to ($\Delta_u = 0$, $\Delta_b = 1.0$) and ($\Delta_u = 1.0, \Delta_b = 0.0$) have been obtained. The results, shown in Fig. 3, indicate that the critical extinction condition is more sensitive to the downstream loss. This result is in qualitative agreement with the prediction made earlier based on phenomenological arguments [9]. As a result of the negligible thickness of the reaction zone, radiative loss from this zone and the relatively colder upstream preheat zone is small. However, downstream of the reaction zone, reduced temperatures enhance conductive heat loss resulting in stronger dependence of the extinction condition on downstream temperature gradients.

The results show that the influences of the loss from each side of the flame are nearly additive (Fig. 3). They agree with those predicted by the laminar flame theory with volumetric heat loss, which shows that the influences of heat loss on the burning rate occur through the perturbation of the downstream temperature from its adiabatic value [10].

In generating the results shown in Figs. 2 and 3, a large value of $\Delta_j = 1$ has been used. In realistic situations the Δ_j's are smaller; in fact rough estimates [3] for small-scale flames with a moderate amount of sooting show that they are of the order of 10^{-6}–10^{-5}. In view of the small changes in the extinction Damköhler

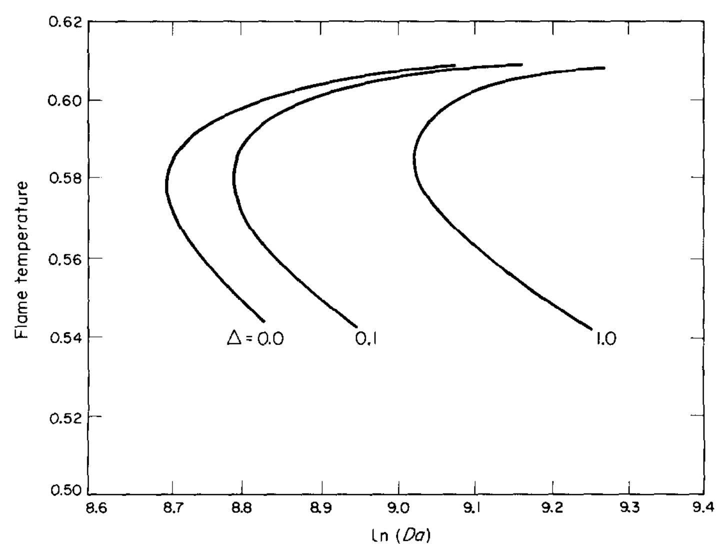

FIG. 2. Extinction curves for various values of radiative loss parameter Δ, with $\alpha = 0.6, \beta = 0.01, T_\infty = 0.02, T_a = 120T_\infty$.

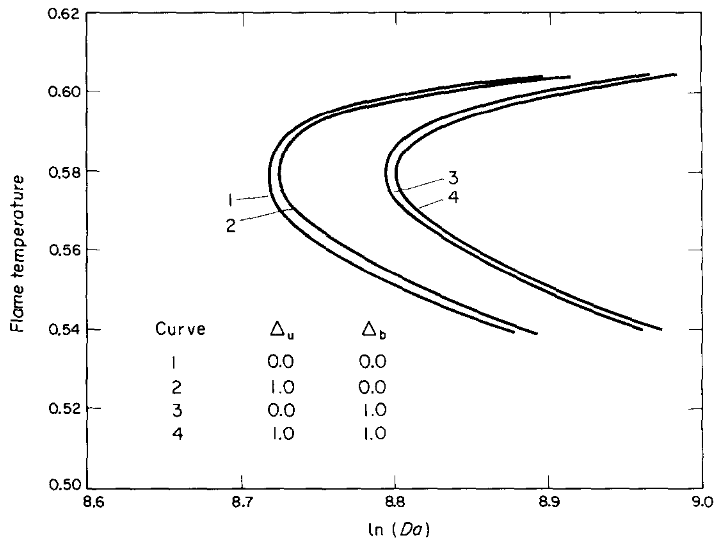

FIG. 3. Extinction curves showing the influences of downstream vs upstream radiative heat loss, with $\alpha = 0.6$, $\beta = 0.01$, $T_\infty = 0.02$, $T_a = 120T_\infty$.

number with substantial variations in Δ_j, it is then clear that radiative heat loss is effective in causing extinction, as compared with flame stretch through Damköhler number variations as well as downstream conductive heat loss. By further suppressing downstream conductive heat loss by analyzing the symmetrical double flame situation in the Appendix, we finally arrive at the conclusion that flame stretch is the dominant mode in effecting extinction. Thus only in the complete absence of flame/flow nonuniformity will radiative loss become important.

In view of the above result, it may then be suggested that radiative loss has negligible effect on the extinction of the rich propane/air flame of Ishizuka and Law [2] as well as Tsuji and Yamaoka [11]. The fact that the double flames fail to merge at extinction may simply indicate that the diffusional stratification effect is still not strong enough. Indeed, by using butane/air mixtures which can induce stronger diffusional stratification, Sato [12] was able to observe complete merging of the double flame at extinction.

6. CONCLUSIONS

Extinction of laminar counterflow premixed flames in the presence of volumetric radiative heat loss is analyzed. An explicit formula for evaluation of the critical Damköhler number at extinction is determined. It is shown that influences of radiative loss are secondary, and mainly felt through the reduced flame temperatures, which result in translation of the extinction curves towards larger Damköhler numbers.

The study includes analysis of both single- and double-flame situations in order to assess the influence of downstream conductive and radiative heat losses on the extinction conditions. In symmetric double-flame situations, the radiation effect is more significant since it is the only possible mode of downstream heat loss. Also, influences of downstream vs upstream radiative losses on the extinction conditions are found to be different; the extinction condition is more sensitive to downstream loss. The combined effects of downstream and upstream losses are nearly additive. A critical maximum value of the downstream radiative loss parameter is identified above which flame propagation is not possible.

Our results also show that except for massively radiating flames, radiative heat loss is relatively unimportant in affecting flame extinction as compared with flame stretch. Since in realistic situations a flame is invariably curved and/or situated in a nonuniform flow field, the importance of stretch in considering extinction is again demonstrated [4].

The final point to note is that while the present steady-state analysis shows whether a steady flame can or cannot be established, the dynamic process of extinction can only be described by a complete transient analysis of the situation. From a practical point of view, however, an extinguishability analysis like the present one is frequently adequate in assessing the reactivity of a given flow/mixture system.

Acknowledgement—This work was supported by NASA-Lewis under grant Nos. NAG-3-53 and NAG-3-361.

REFERENCES

1. J. DeRis, Fire radiation—a review, *Proc. 17th Int. Symp. Combust.*, pp. 1003–1016 (1979).
2. S. Ishizuka and C. K. Law, An experimental investigation on extinction and stability of stretched premixed flames, *Proc. 19th Int. Symp. Combust.*, pp. 327–335 (1982).
3. S. H. Sohrab, A. Liñán and F. A. Williams, Asymptotic theory of diffusion flame extinction with radiant loss from the flame zone, *Combust. Sci. Technol.* **28**, 143–154 (1982).

4. B. Lewis and G. Von Elbe, *Combustion Flames and Explosions of Gases*. Academic Press, New York (1967).
5. F. A. Williams, *Combustion Theory*, p. 198. Addison-Wesley, Reading, Massachusetts (1965).
6. R. Siegel and J. R. Howell, *Thermal Radiation Heat Transfer*, pp. 708–730. McGraw-Hill, New York (1972).
7. S. S. Penner and D. B. Olfe, *Radiation and Reentry*, pp. 144–165, 192. Academic Press, New York (1968).
8. A. Liñán, The asymptotic structure of counterflow diffusion flames for large activation energies, *Act. Astronautica* **1**, 1007–1039 (1974).
9. E. Mayer, A theory of flame propagation limits due to heat loss, *Combust. Flame* **1**, 438–452 (1957).
10. G. Joulin and P. Clavin, Linear stability analysis of nonadiabatic flames, *Combust. Flame* **35**, 139–153 (1979).
11. H. Tsuji and I. Yamaoka, Structure and extinction of near-limit flames in a stagnation flow, First Specialists Meeting (Int.) of the Comb. Inst., Tome I, Bordeaux, pp. 111–116 (1981).
12. J. Sato, Effects of Lewis number on extinction behavior of premixed flames in a stagnation flow, *Proc. 19th Int. Symp. Combust.*, pp. 1541–1548 (1982).

APPENDIX

DOUBLE-FLAME ANALYSIS

Extinction of the flame studied in the text is induced by heat loss through both radiation as well as to the cold inert stream. We now suppress the latter loss so as to demonstrate the possibility and the properties of extinction purely through radiative heat loss. Experimentally this situation can be realized by using identical opposed jets which result in a double-flame configuration [2]. Because of symmetry, the stagnation surface becomes perfectly adiabatic when the radiation zone is situated away from it. The conservation equations [equations (8) and (9)], will remain the same and only the boundary conditions in equation (10) are modified to the following forms

$$\begin{aligned} x = 1 \text{ and } 0: &\quad T-T_\infty = Y_F-1 = Y_O-\alpha = 0, \\ x = 1/2: &\quad \frac{dT}{dx} = Y_O = Y_F+\alpha-1 = 0. \end{aligned} \tag{A1}$$

As a result of symmetry, only the semi-infinite region $0 \leqslant x \leqslant 1/2$ needs to be considered.

Under the new boundary conditions, the downstream temperature distribution outside of the radiative zone corresponding to equation (17) assumes the modified form

$$T = T_0, \quad 1/2 \leqslant x < x_f, \tag{A2}$$

where T_0 is not known and must be determined. In view of equation (A2), a similar procedure leading to equation (18) will result in the total radiative loss given by

$$q = \frac{\alpha}{x_f} - \frac{T_f - T_\infty}{x_f}. \tag{A3}$$

From the analysis of the radiation zone which follows that stated previously, in Section 3, and with appropriate matching of the new downstream temperature gradient we obtain

$$\sqrt{(2\Delta_b)} + \left\{ 2\Delta_u + \left(\frac{T_f - T_\infty}{x_f} \right)^2 \right\}^{1/2} = \frac{\alpha}{x_f}. \tag{A4}$$

The above equation relates the nonadiabatic flame temperature and location to the radiative loss parameter Δ_j. The temperature gradient downstream of the reaction zone is now

$$G^+ = \sqrt{(2\Delta_b)}. \tag{A5}$$

Analysis of the reaction zone structure is similar to that presented in Section 4 with the parameter G^+ replaced by the modified value in equation (A5). From equations (36), (A5) and (53), the following expression, which relates the Damköhler number to T_f, x_f and Δ_j, is obtained

$$Da = \frac{1}{4\pi} \exp(-z_f^2) \left(\frac{\alpha T_a}{x_f T_f^2} \right)^2 \left(\frac{1}{1-\alpha} \right) \exp(T_a/T_f) \times \exp\left[-n \left(\frac{x_f}{\alpha} \right) \sqrt{(2\Delta_b)} \right], \tag{A6}$$

where the fuel mass fraction at the flame is $(1-\alpha)$. Plots of Da as a function of T_f for various values of the parameter Δ_j are similar to those shown in Fig. 2 for the single-flame analysis. However, in the absence of downstream conductive heat loss, the radiative loss from burnt gas expressed through Δ_b in equation (A6) attains more significance.

Examination of the downstream temperature T_0 requires analysis of the radiative zone. From the first integral of equation (23) from $\xi \to +\infty$ to ξ we obtain

$$\frac{d\phi}{d\xi} = (2\Delta_b e^{\phi})^{1/2}. \tag{A7}$$

In determining equation (A7), use of the matching condition to the downstream outer solution (A2) has been made. The solution of equation (A7) which satisfies the condition $\phi(0) = 0$ is

$$\phi = -2 \ln [1 - (\Delta_b/2)^{1/2} \xi]. \tag{A8}$$

As x approaches 1/2, corresponding to $\xi \simeq (0.5 - x_f)(\gamma_{bf}/T_f)$, equation (A8) gives the limiting temperature expressed as

$$T_0 \cong T_f - \frac{T_f}{\gamma_{bf}} \ln \left[1 - (0.5 - x_f) \frac{\gamma_{bf}}{T_f} (\Delta_b/2)^{1/2} \right]. \tag{A9}$$

Therefore the perturbation of downstream temperature from the flame temperature is small, $O(1/\gamma_{bf})$, as is anticipated for small Δ_b. A schematic diagram of the temperature distribution for the double-flame situation is shown in Fig. 1(b).

EXTINCTION DES FLAMMES PREMELANGEES PAR EXPANSION ET PERTE RADIATIVE

Résumé— L'extinction des flammes prémélangées laminaires par expansion et perte radiative est étudiée pour le modèle d'une combustion en jet opposé à contrecourant en utilisant la technique de développement asymptotique, pour les mécanismes de pertes thermiques radiatives très sensibles à la température et des cinétiques de réaction à grande énergie d'activation. Des expressions explicites du nombre critique de Damköhler à l'extinction sont obtenues et l'influence des pertes thermiques de l'amont à l'aval est précisée. Des résultats montrent que l'expansion exerce une plus grande influence que la perte radiative sur l'extinction de la flamme.

DAS AUSLÖSCHEN VON VORGEMISCHTEN FLAMMEN DURCH AUSDEHNUNGS- UND WÄRMESTRAHLUNGSVERLUSTE

Zusammenfassung—Das Auslöschen von vorgemischten Flammen durch Ausdehnungs- und Wärmestrahlungsverluste wurde für das Modell der Gegenstrom-Gegenstrahl-Verbrennung untersucht. Dabei wurde für die stark temperaturempfindlichen Vorgänge beim Wärmeverlust durch Strahlung und bei der Reaktionskinetik mit hoher Aktivierungs-Energie das Verfahren der asymptotischen Entwicklung angewandt. Für die kritische Damköhler-Zahl beim Auslöschen der Flamme wurde eine explizite Gleichung hergeleitet und der Einfluß der stromauf gegenüber den stromab auftretenden Wärmeverlusten abgeschätzt. Die Ergebnisse zeigen, daß der Ausdehnungsverlust einen viel größeren Einfluß auf das Auslöschen der Flamme hat als der Wärmestrahlungsverlust.

ВЛИЯНИЕ ЛУЧИСТЫХ ТЕПЛОПОТЕРЬ И ТЕПЛООТДАЧИ В ОКРУЖАЮЩУЮ СРЕДУ НА ЗАТУХАНИЕ ПЛАМЕН ПРЕДВАРИТЕЛЬНО СМЕШАННЫХ ГАЗОВ

Аннотация—Изучено влияние теплопотерь излучением и теплоотдачей в окружающую среду на затухание ламинарных пламен предварительно перемешанной горючей смеси для модельной задачи горения в п противопотоке методом сращиваемого асимптотического разложения лучистых теплопотерь и теплоотдачи в процессе химической реакции высокой активности. Получены выражения в явном виде для критического числа Дамкёлера при затухании и оценено влияние потерь тепла вверх по потоку в сравнении с потерями вниз по потоку. Результаты показывают, что теплоотдача в окружающую среду оказывает более сильное влияние на затухание пламени, чем потери на излучение.